THREE CS-BASED BEAMFORMERS FOR SINGLE SNAPSHOT DOA ESTIMATION

Stefano Fortunati[#], Raffaele Grasso[*], Fulvio Gini[#], Maria S. Greco[#], Kevin LePage[*]*

[#]Dipartimento di Ingegneria dell'Informazione, University of Pisa, via G. Caruso 16, 56122, Italy.
[*]CMRE, Viale San Bartolomeo 400, 19126 La Spezia.

ABSTRACT

In this work, the estimation of the Directions of Arrival (DOAs) of multiple source signals from a single observation vector is considered. In particular, the estimation, detection and super-resolution performance of three algorithms based on the theory of Compressed Sensing (the classical l_1-minimization or LASSO, the fast smooth l_0-minimization, and the SPICE algorithm) are analyzed and compared with the classical Fourier beamformer. This comparison is carried out using both simulated data and real sonar data.

Index Terms: *Compressive Sensing, DOA estimation, Fourier Beamformer, Super-resolution, Sonar.*

1. INTRODUCTION

The problem of estimating the Directions of Arrival (DOAs) of a certain number of sources has been an active research area for decades [1], [2], with a huge variety of applications. Due to its fundamental importance, many DOA estimation algorithms have been proposed in the literature. In brief, the estimation methods can be categorized in two large classes: the non-parametric (spectral-based) algorithms and the parametric algorithms [2]. The non-parametric algorithms (e.g. Fourier and Capon) exploit some spectrum-based function of the parameters to be estimated, e.g. the DOAs. The parametric techniques, e.g. MUSIC, Deterministic Maximum Likelihood (DML) [3] and Stochastic ML (SML) [4] algorithms, on the other hand, fully exploit the statistical characterization of the measurement model. The latter approach often guarantees higher estimation performance than the spectral-based methods, albeit at the expense of an increased computational complexity.

However, almost all these algorithms have to work in the so-called "asymptotic region", i.e., they need high SNR values and a large number of snapshots in order to provide reliable estimates. In some applications, e.g. sonar applications, due to physical constraints, only a very small number of snapshots or, in the worst case, a single snapshot is available for DOA estimation. In the single snapshot scenario, adaptive algorithms (*e.g.* Capon, MUSIC, DML and SML), that rely on an estimate of the noise covariance matrix, cannot be applied. Recently, new spectral-based estimation algorithms, based on the emerging field of the Compressed

Sensing (CS) theory have been proposed [5]. In this paper, the statistical properties of three CS-based beamformers (CSB), the l_1-minimization or LASSO, the fast smooth l_0-minimization, and the SPICE algorithm will be investigated. The analysis is carried out in the single snapshot scenario, which is of practical relevance in many sonar applications. The focus here is on three statistical properties: (*i*) the efficiency in the DOA estimation; (*ii*) the Receiver Operating Characteristic Curves (ROC); and (*iii*) the resolution capability. The simulation results will be verified also using a real sonar dataset.

2. THE MEASUREMENT MODEL

Assume a Uniformly Linear Array (ULA) of N omnidirectional sensors spaced by d and K narrowband sources impinging on the array from conic angles $\{\bar{\theta}_k\}_{k=1}^K$. Moreover, suppose that only one snapshot is collected at the output of the matched filter for each range cell. The vector snapshot can be modeled as [1], [2]:

$$\mathbf{y} = \mathbf{s} + \mathbf{n} = \sum_{k=1}^K \rho_k \mathbf{v}(\bar{\nu}_k) + \mathbf{n}, \qquad (1)$$

where $\bar{\nu}_k = d/\lambda_0 \sin\bar{\theta}_k$ is the spatial frequency, λ_0 is the wavelength of the transmitted signal, $\mathbf{v}(\bar{\nu}_k) = [1, \exp(j2\pi\bar{\nu}_k), \cdots, \exp(j2\pi(N-1)\bar{\nu}_k)]^T$ is the $N\times1$ steering vector at the direction $\bar{\theta}_k$ and $\mathbf{n}$ is the complex $N\times1$ measurement noise vector (either Gaussian or non-Gaussian) with zero-mean and covariance matrix $\mathbf{C}$. Finally, $\{\rho_k\}_{k=1}^K$ are complex scalars, each of which can be modeled as an unknown factor of the form $\rho_k = |\rho_k|e^{j\varphi_k}$, where the phase φ_k is a uniformly distributed random variable (r.v.) in $[0, 2\pi)$ and (*i*) the magnitude $|\rho_k|$ is a deterministic parameter, or (*ii*) the magnitude $|\rho_k|$ is a Rayleigh r.v. with power $E\{|\rho_k|^2\}=2\sigma_\rho^2$, which is equivalent to assuming that ρ_k is a complex, zero-mean, Gaussian r.v. with variance σ_ρ^2, *i.e.* in shorthand notation $\rho \in \mathcal{CN}(0, \sigma_\rho^2)$.

3. BRIEF DESCRIPTION OF THE ALGORITHMS

In this section, the classical Fourier beamformer (FB) and the three CSB are described and compared.

3.1 The Fourier Beamformer

Under the white noise and single deterministic signal model assumptions, the ML estimator for $\bar{v}$ is given by the location of the maximum of the data Periodogram [1], [2]:

$$\hat{v}_F = \arg\max_v \left| \sum_{n=0}^{N-1} y_n e^{-j2\pi nv} \right|^2 = \arg\max_v p_F(v) . \quad (2)$$

This estimator is known as the Fourier beamformer (FB). $p_F(v)$ is usually evaluated using the Fast Fourier Transform (FFT) on a discrete set of spatial frequencies $\Upsilon = \{v_j\}_{j=1}^{|\Upsilon|}$, where $|\Upsilon|$ is the cardinality of the set Υ. Generally, $|\Upsilon|$ is chosen to be equal to N as a consequence of the low resolution of the Fourier beamformer.

3.2 The CS formulation of the DOA estimation problem

As shown in [5], the measurement model in eq. (1) can be recast in a "sparse" representation by defining an overcomplete dictionary $\mathbf{A}(\Omega)$ of steering vectors evaluated over a set of possible spatial frequencies $\Omega = \{v_1, \ldots, v_G\}$. In general, the true source spatial frequencies could not belong to this set, since Ω is arbitrarily chosen without any a priori knowledge on $\{\bar{v}_k\}_{k=1}^K$. However, in order to guarantee a coherence between the signal in eq. (1) and the CS-like signal model, we assume that $\{\bar{v}_k\}_{k=1}^K \subset \Omega$. The effects of the violation of this assumption (called *off-grid effects*) are discussed later on, in Section 4.1. Then, the source signal has to be recast as a $G \times 1$ column vector $\mathbf{x}$ where the gth entry, i.e. x_g, is equal to ρ_g if the source has a spatial frequency equal to v_g and zero otherwise. Since the cardinality G of the dictionary, i.e. the number of grid points used to cover the spatial frequency space, is much larger than the number K of possible sources, then the vector $\mathbf{x}$ is sparse. Finally, the measurement model of eq. (1) can be recast in the well-known linear CS measurement model:

$$\mathbf{y} = \mathbf{A}(\Omega)\mathbf{x} + \mathbf{n}. \quad (3)$$

Estimating the spectrum-like function $p_{CS}(\Omega) = |\hat{\mathbf{x}}(\Omega)|^2$ from eq. (3), is equivalent to estimating the spatial energy as a function of the set of assumed spatial frequencies Ω. Then, by assuming to have a single source in the scenario ($K=1$), a CS-based DOA estimator is given by:

$$\hat{v}_{CS} = \arg\max_\Omega |\hat{\mathbf{x}}(\Omega)|^2 = \arg\max_\Omega p_{CS}(\Omega) . \quad (4)$$

In the following, three different methods to estimate $\mathbf{x}$ from the measurement vector $\mathbf{y}$ are discussed and compared.

3.2.1 The l_1-minimization (L1) algorithm

In its most general form, finding an estimate of $\mathbf{x}$, from the measurements in eq. (3), belongs to the well-known class of constrained optimization problem that can be solved using a LASSO (Least Absolute Shrinkage and Selection Operator) solver (see e.g. [6]):

$$\hat{\mathbf{x}}_{CS}(\Omega) = \arg\min_{\mathbf{x} \in \mathbb{C}^G} \|\mathbf{x}\|_1 \quad \text{s.t.} \|\mathbf{A}(\Omega)\mathbf{x} - \mathbf{y}\|_2 \leq \delta . \quad (5)$$

One of the big advantages of the LASSO algorithm is that it should promote sparse solutions irrespective of the particular noise distribution function. On the other hand, the LASSO solver requires the setting of many additional parameters that have to be selected heuristically by the user. An example of a critical parameter is the threshold value δ in the constraint of eq. (5). Clearly, δ is a function of the noise covariance matrix $\mathbf{C}$ that is, in general unknown.

3.2.2 The smooth l_0-minimization (SL0) algorithm

The SL0 algorithm is a suboptimal algorithm based on a continuous approximation of the l_0 norm [7]. Instead of a problem similar to the one in eq. (5), in [7] the authors propose to solve the following problem:

$$\hat{\mathbf{x}}(\Omega) = \arg\min_{\mathbf{x} \in \mathbb{C}^G} F(\mathbf{x}) \quad \text{s.t. } \mathbf{A}(\Omega)\mathbf{x} = \mathbf{y} \quad (6)$$

where F is some continuous function that approximates the l_0 norm. Of course, the SL0 is a suboptimal algorithm for the DOA estimate. In fact, as can be seen from eq. (6), the SL0 algorithm does not take into account the measurement noise. However, the SL0 algorithm has two advantages with respect to the classical LASSO algorithm: (*i*) the numerical minimization algorithm (a gradient-based algorithm) is very fast and (*ii*) the SL0 algorithm requires the choice of a very small number of critical parameters.

3.2.3 The SPICE algorithm

The SPICE (SParse Iterative Covariance-based Estimator) algorithm was first derived for the single snapshot case [8] and then generalized to the multi-snapshot case [9]. The SPICE algorithm has a different and stronger statistical foundation with respect to the L1 or SL0 algorithms and it does not require any difficult and heuristic selection of parameters, since they are jointly estimated during the iteration. Suppose that the noise vector $\mathbf{n}$ in the measurement model in eq. (3) is a zero-mean, Gaussian distributed complex random vector, with diagonal covariance matrix $\mathbf{C} = \text{diag}(\sigma_1^2, \ldots, \sigma_N^2)$. By using the same assumptions introduced in Sec. 2, the covariance matrix of the measurement vector $\mathbf{y}$ can be expressed as:

$$\mathbf{R} = E\{\mathbf{y}\mathbf{y}^H\} = \sum_{g=1}^G p_g \mathbf{v}(v_g)\mathbf{v}(v_g)^H + \text{diag}(\sigma_1^2, \ldots, \sigma_N^2), (7)$$

where p_g is equal to (*i*) $|x_g|^2$ for a deterministic signal model and (*ii*) $2\sigma_\rho^2$ for the random signal model. The parameters to be estimated are then the spectrum-like function $p_{SPICE}(\Omega) \triangleq \{p_g\}_{g=1}^G$ and the noise covariance matrix $\mathbf{C}$. The joint estimate of these parameters is obtained by minimizing the following covariance-based objective function [8]:

$$\left(p_{SPICE}(\Omega), \hat{\mathbf{C}}\right) = \arg\min_{\left(\{p_g\}_{g=1}^{|\Omega|}, \{\sigma_i^2\}_{i=1}^N\right) \in \mathbb{R}_0^+} \left\| \mathbf{R}^{-1/2}\left(\mathbf{y}\mathbf{y}^H - \mathbf{R}\right) \right\|_F^2, \quad (8)$$

where $\| \cdot \|_F$ is the Frobenius norm. The minimization problem in eq. (8) has an iterative closed form solution [8]. Interestingly, even if they have been derived from two completely different perspectives, the SPICE and the L1 algorithms are strictly related. This connection has been extensively discussed in [10].

4. STATISTICAL PERFORMANCES

In this section, we investigate the estimation, detection and super-resolution performance of the CSB DOA estimators in terms of $\text{RMSE} = E\{(\bar{v} - \hat{v})^2\}^{1/2}$, ROC curves and Probability of Resolution (see Sect. 4.3) respectively. The single snapshot scenario is assumed and two different kinds of disturbance are used: Gaussian white noise and Gaussian white noise plus Gaussian spatially-correlated clutter. In particular, the clutter is modeled as an autoregressive (AR) process of order 1, so the covariance matrix of the disturbance **n** is:

$$\mathbf{C} = \begin{cases} \text{a) } \sigma_n^2 \mathbf{I}, & \text{white noise only} \\ \text{b) } \sigma_n^2 \mathbf{I} + \sigma_c^2 \mathbf{Q}(\xi), & \text{noise plus clutter} \end{cases}. \quad (9)$$

In all our simulation, we assume an array of N=32 elements, while the number of grid-points is $|\Omega|=|\Upsilon|=G$. Moreover, the nominal value of the target spatial frequency $\bar{v}$ is chosen uniformly at random in [-0.5,0.5] and the number of independent Monte Carlo runs is 10^4.

4.1 RMSE on DOA estimation

In Fig. 1, the comparison among the RMSE of the four beamformers and the Cramer-Rao Lower Bound (CRLB) is shown for the spatially-correlated clutter scenario (eq. (9.b)) and a deterministic source model. The CRLB has already been derived as [11]:

$$\text{CRLB}(\bar{v}) = \left(2|\rho|^2 \mathbf{d}^H \mathbf{C}^{-1/2} \mathbf{\Sigma} \mathbf{C}^{-1/2} \mathbf{d} \right)^{-1} \quad (10)$$

where $\mathbf{\Sigma} = \mathbf{I} - \mathbf{C}^{-1/2} \mathbf{v} (\mathbf{v}^H \mathbf{C}^{-1} \mathbf{v})^{-1} \mathbf{v}^H \mathbf{C}^{-1/2}$, $\mathbf{d} = \partial \mathbf{v} / \partial \bar{v}$ and in the steering vector **v**, the dependence of the actual spatial frequency is omitted for notation simplicity. The measurement model in eq. (3) is assumed with the following parameters: $G=2^{10}$, $\sigma_n^2=1$, $[Q(\xi)]_{ij}=(\xi^{|i-j|})^*$, $\xi=0.98e^{j\vartheta}$ where ϑ is a uniformly distributed random variable in $[0,2\pi]$ and σ_c^2 is chosen accordingly to the given Clutter-to-Noise Ratio (CNR) value: $\sigma_c^2=\text{CNR}\sigma_n^2$. In this simulation CNR = 15db. Finally, the Signal-to-Interference-plus-Noise Ratio can be defined as $\text{SINR}=|\rho|^2/(\sigma_n^2+\sigma_c^2)$.

From Fig. 1 we get that the FB and the CSBs have similar performance in terms of RMSE. It can also be noted that, below 25dB of SINR (and for a CNR = 15db), all the estimators are in the "low SNR" region where the CRLB is not tight. Beyond 25dB, the estimators are close to the CRLB. However, for high SINR values, the so called *off-grid effects* become evident. They are bias errors in the DOA estimation that arise when the nominal target spatial frequency $\bar{v}$ does

not belong to the set Υ for the FB and to Ω for the CSBs. Of course, the residual bias depends on the "thinness" of the grid and it is upper bounded by $1/2G$. This value is achieved when $\bar{v}$ falls exactly between two grid-points.
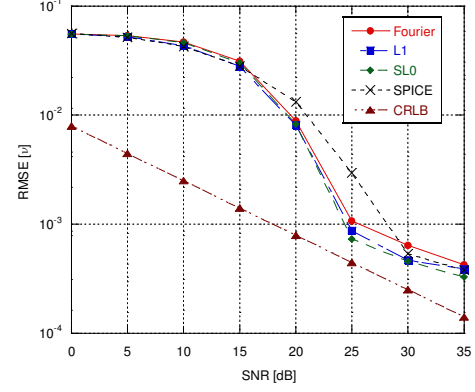

Fig. 1. RMSE on DOA estimation

4.2 ROC evaluation

The Receiver Operating Characteristic (ROC) curves show the Probability of Detection (PD) as a function of the Probability of False Alarm (PFA). In Fig. 2 the comparison among the ROC curves of the FB and of the three CSBs in the spatially-correlated clutter scenario (eq. (9.b)) is presented. The random signal model is used in which ρ is assumed to be a zero-mean complex Gaussian random variable with $\sigma_\rho^2=\text{SINR}\cdot(\sigma_n^2+\sigma_c^2)$.

Here, SINR=-10dB, 0dB, and 10dB, and G=180. In this case, all the three CSBs outperform the classical FB. In fact, for each PFA, the PD provided by each CSB is always higher than the one provided by the FB. In particular, the SPICE and the L1 algorithms have the best detection performance, especially at low SINR values.
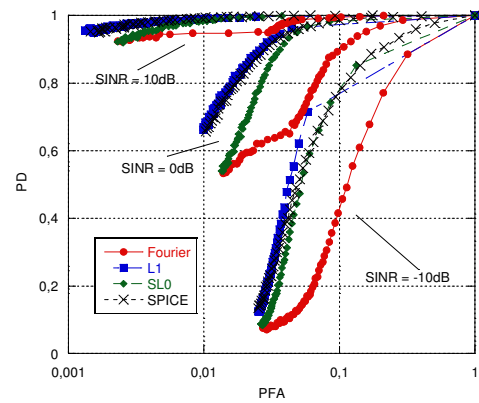

Fig. 2. ROC curves case for three different SINRs.

4.3 The super-resolution property

The FB suffers from the Rayleigh resolution limit, which is independent of the SNR. In particular, for an ULA of N array elements, the Rayleigh resolution limit, *i.e.* the

beamwidth in the spatial frequency space, defined as the full width of the mainlobe at the half-power level, is $\Delta v = 0.886/N$. In some recent publications ([5],[12]), it is shown that the CSBs are able to achieve the super-resolution even in the single-snapshot case. In [12], the super-resolution limit for a CSBs is derived as $\overline{\Delta v} = \exp(-C_d N/K)$ where C_d is a given constant. Then, while the Rayleigh resolution limit decreases as N^{-1}, the CS super-resolution limit decreases as $\exp(-\alpha N)$. The aim of this section is to compare the super-resolution capability of the L1, SL0 and SPICE algorithms with the FB. A white noise scenario (eq. (9.a)) and a random signal model are assumed. The analysis is performed by evaluating the probability of resolution, P_{res}. In [12] and [13], the following random inequality is used to define a super-resolution event:

$$\gamma(v_1, v_2) \triangleq \frac{1}{2}\left[p_{CS}(v_1) + p_{CS}(v_2)\right] - p_{CS}(v_m) > 0, \quad (11)$$

where $v_m = (v_1 + v_2)/2$ and p_{CS} is the generic CS spectrum-like function. Two equipowered sources located at spatial frequencies v_1 and v_2 are said to be resolvable if the inequality in eq. (11) holds true and to be irresolvable otherwise. This problem can then be seen as a binary decision problem, where γ is the decision statistic. The probability of resolution can then be defined as $P_{res} = \Pr\{\gamma > 0\}$. In Fig. 3, P_{res} is evaluated as a function of the source separation in the spatial frequency domain for SNR=10dB and $G=2^9$. The frequency separation, denoted as $\Delta = 2l/G$ for $l=1,2,\dots,L<G$ is defined with respect to $v_m = 0.3$ so that the spatial frequencies of the two sources are given by $v_1 = v_m - \Delta/2$ and $v_2 = v_m + \Delta/2$. From Fig. 3, it is clear that the P_{res} of the CSBs is always higher than that of the FB. We observe also that the P_{res} of SPICE is close to 1 also for Δ below the Rayleigh limit, which is plotted in red. Clearly, by decreasing Δ, P_{res} also decreases. The SPICE algorithm is the one that provides the best P_{res}.
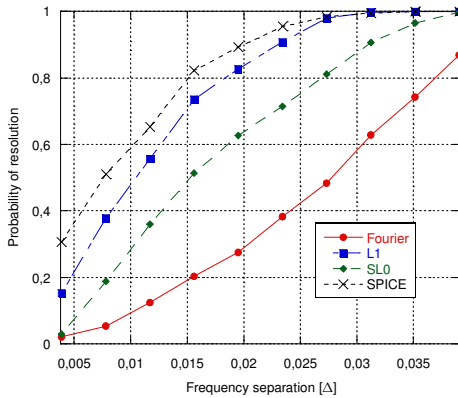

Fig. 3. P_{res} as function of source spatial frequency separation.

5. REAL DATA ANALYSIS

Data collected during the Co-Operative littoraL Asw Behaviour (COLLAB) 2013 experiment are used to test CSB

algorithms on real acoustic array measurements. The experiment has been conducted by CMRE in La Spezia waters, Italy, from 29 June to 7 July 2013. During the experiment, a bistatic system has been used with the transmitter, at fixed known position, that insonifies a surveillance region with a predefined pulse repetition interval (PRI) by transmitting a frequency modulated chirp signal. An underwater towed target (an echo repeater) was used to test detection and tracking performance by a 32 element hydrophone array towed by an Autonomous Underwater Vehicle (AUV). Received scan data are processed to compare CSBs against the FB. Preprocessing of the received data includes base band conversion, complex matching filtering and normalization for the attenuation profile.
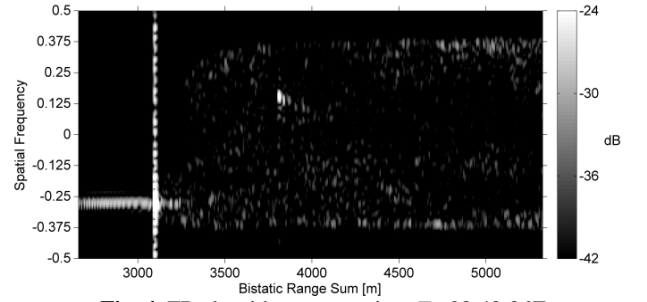

Fig. 4. FB algorithm at scan time T_s=08:49:36Z.

The complex normalized data have been beamformed using a spatial frequency grid of 180 points for each range cell of a scan. Fig. 4 shows the results of the FB at scan time T_s=08:49:36Z. The map scale represents normalized power in dB with respect to the direct blast maximum power. The target is visible at a bistatic range sum (BRS) of 3809 m and spatial frequency between 0.125 and 0.25. The direct blast from the transmitter is visible at a BRS of 3093 m and spatial frequency -0.27. However, the results are affected by the so-called left-right ambiguity [14] of linear arrays, so the real target spatial frequency can be actually the opposite of the one observed in the map. The disambiguation is achieved by using the target and the AUV navigation data, the transmitter position and the array parameters to locate the target within the map. Fig. 5 shows the L1, the SL0 and the SPICE beamformers at scan time T_s with improved resolution and side lobe levels with respect to the classical FB.

6. CONCLUDING REMARKS

In this paper, three CSBs, *i.e.* the L1 (or LASSO), the SL0 and the SPICE algorithms, have been analyzed and compared with the classical FB for target DOA estimation in a single-snapshot scenario. The DOA estimation accuracy, the detection performance, and the resolution capability of the three algorithms were analyzed and compared against the classical FB algorithm. Regarding the estimation performance, the three CSBs and the FB present fairly similar performance. As far as the detection performance is concerned, in the spatially correlated noise scenario the three CSBs outperform the classical FB. In particular, the SPICE

and the L1 algorithms have the best detection performance, especially at low SNR values. Concerning the resolution capability, the simulations have shown that the SPICE algorithm has the best super-resolution performance in terms of P_{res}.
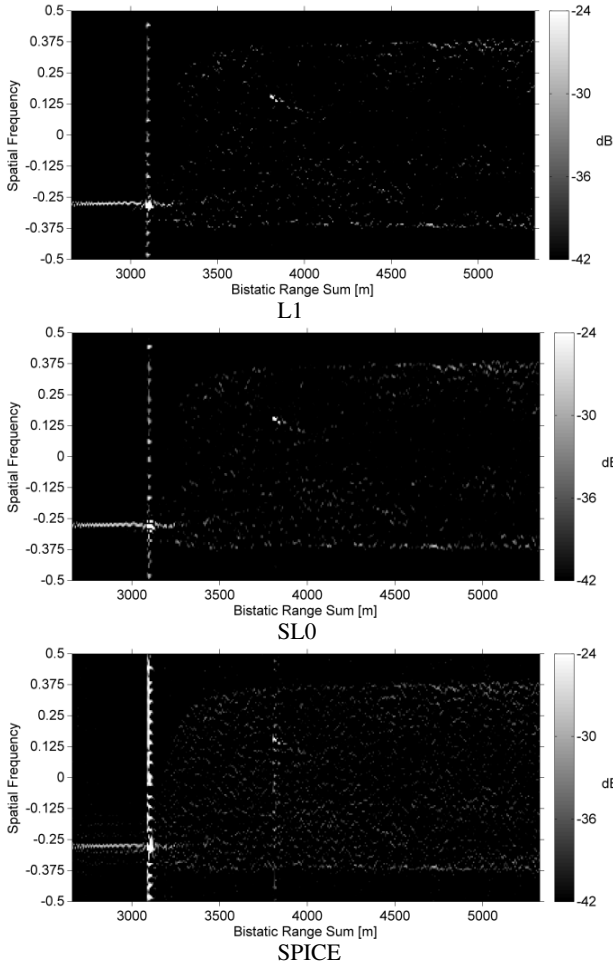

L1

SL0

SPICE

Fig. 5. CSB at T_s=08:49:36Z..

The reduction of the secondary lobes by the CS-based algorithms, hence the reduction of the PFA, is clear by comparing the range-spatial frequency maps at the output of the beamformers when using real sonar data. From the same maps, the super-resolution capability of the CSBs has been verified, as well. Concerning the processing time, the SL0 algorithm is one or even two order of magnitude faster than the SPICE and the L1 algorithm. Since, in many practical applications, a low processing time is a stringent requirement, the SL0 algorithm could represent a good tradeoff between the statistical optimality and the practical implementation. Future research efforts will explore the application of the proposed CSBs to the multi-snapshot case. Moreover, a deeper comprehension of the statistical properties of the CSBs in different noise and clutter distributions

(e.g. the widely known compound-Gaussian distributions) has to be developed.

REFERENCES

[1] H. Van Trees, *Optimum Array Processing (Part IV)*, John Wiley & Sons, 2002.

[2] H. Krim, M. Viberg, "Two decades of array signal processing research: the parametric approach," *IEEE Signal Process. Mag.*, vol. 13, no. 4, pp. 67-94, Jul 1996.

[3] J. F. Bohme, "Estimation of source parameters by maximum likelihood and nonlinear regression," *IEEE ICASSP '84*, vol. 9, pp.271 - 274, Mar 1984.

[4] A. G. Jaffer, "Maximum likelihood direction finding of stochastic sources: a separable solution," *IEEE ICASSP '88*, vol. 5, pp. 2893-2896, 11-14 Apr 1988.

[5] D. Malioutov, M. Cetin, A. S. Willsky, "A sparse signal reconstruction perspective for source localization with sensor arrays," *IEEE Trans. Signal Process.*, vol. 53, no. 8, pp. 3010-3022, Aug. 2005.

[6] R. Tibshirani, "Regression shrinkage and selection via the Lasso," *Journal of the Royal Statistical Society, Series B*, no. 58 vol. 1, pp. 267 – 288, 1996.

[7] H. Mohimani, M. Babaie-Zadeh, C. Jutten, "A Fast Approach for Overcomplete Sparse Decomposition Based on Smoothed Norm," *IEEE Trans. on Signal Process.*, vol.57, no.1, pp.289-301, Jan. 2009.

[8] P. Stoica, P. Babu, J. Li, "New Method of Sparse Parameter Estimation in Separable Models and Its Use for Spectral Analysis of Irregularly Sampled Data," *IEEE Trans. on Signal Process.*, vol. 59, no.1, pp. 35-47, Jan. 2011.

[9] P. Stoica, P. Babu and J. Li, "SPICE: A Sparse Covariance-Based Estimation Method for Array Processing," *IEEE Trans. on Signal Process.*, vol. 59, no. 2, pp. 629-638, Feb. 2011.

[10] C. R. Rojas, D. Katselis, H. Hjalmarsson, "A Note on the SPICE Method," *IEEE Trans. on Signal Process.*, vol. 61, no. 18, pp. 4545-4551, Sept.15, 2013.

[11] M. Viberg, P. Stoica, B. Ottersten, "Maximum likelihood array processing in spatially correlated noise fields using parameterized signals," *IEEE Trans. on Signal Process.*, vol. 45, no. 4, pp.996-1004, April 1997.

[12] S. Fortunati, R. Grasso, F. Gini, M. S. Greco, "Single snapshot DOA estimation using Compressed Sensing," *IEEE ICASSP 2014*, Florence, Italy, 4-9 May 2014.

[13] Q. T. Zhang, "Probability of resolution of the MUSIC algorithm," *IEEE Trans. on Signal Process.*, vol. 43, no. 4, pp. 978-987, April 1995.

[14] P. Braca, K. LePage, P. Willett, S. Marano, and V. Matta, Particle Filtering Approach to Multistatic Underwater Sensor Networks with Left-Right Ambiguity, *IEEE FUSION 2013*, Istanbul 2013.